CONF-960850--10 ANL/CMT/CP--88969

IDENTIFICATION AND QUANTIFICATION OF PHASES FORMED DURING THE PROCESSING OF $(Bi,Pb)_2Sr_2Ca_2Cu_3O_x$/Ag COMPOSITE CONDUCTORS*

N.N. Merchant, A.K. Fischer, V.A. Maroni
Argonne National Laboratory
Argonne, IL 60439

W.L. Carter and R.D. Parrella
American Superconductor Corporation
Westborough, MA 01581

August 1996

Prepared for presentation at the 1996 Applied Superconductivity Conference, August 25-30, 1996, Pittsburgh, PA.

*Work at Argonne National Laboratory was sponsored by the U.S. Department of Energy, Office of Energy Efficiency and Renewable Energy as part of a DOE program to develop electric power technology, under Contract W-31-109-ENG-38.

DISCLAIMER

IDENTIFICATION AND QUANTIFICATION OF PHASES FORMED DURING THE PROCESSING OF $(Bi,Pb)_2Sr_2Ca_2Cu_3O_x$/Ag COMPOSITE CONDUCTORS

N.N. Merchant, A.K. Fischer, V.A. Maroni, Argonne National Laboratory, Argonne, IL 60439

W.L. Carter and R.D. Parrella, American Superconductor Corporation, Westborough, MA 01581

Abstract--Scanning electron microscopy, energy dispersive X-ray analysis (including X-ray dot mapping), X-ray diffraction and computer-based image analysis have been used to study non-superconducting secondary phases that evolve during the processing of $(Bi,Pb)_2Sr_2Ca_2Cu_3O_x$/Ag composite conductors. These investigations have provided new information and insights about specific alkaline earth cuprates (AECs) and lead-rich phases. We can conclusively identify $(Ca,Sr)_2CuO_3$, $(Ca,Sr)_{14}Cu_{24}O_{41}$, and CuO phases, the alkaline earth plumbates, and a (Bi,Pb)-Sr-Ca-Cu-O 3221 phase with a wide range of Pb/Bi ratios. These techniques also help in differentiating voids from secondary phases and alkaline earth plumbates from the lead-rich 3221 phase.

I. INTRODUCTION

Thermomechanical processing parameters are known to have a dramatic effect on the final electrical performance of silver-clad Bi-2223 superconducting tapes [1,2]. Much recent work has focused on optimizing Bi-2223 phase purity and microstructure [3-9]. Techniques such as scanning electron microscopy (SEM) coupled with energy dispersive X-ray (EDX) analysis, and X-ray diffraction (XRD) have been the most commonly used characterization techniques in studies of the evolution of secondary phases and the superconducting layered phase in Bi-2223/Ag composite conductors.

This paper emphasizes the utility of X-ray dot maps for secondary phase identification and the application of computer image analysis software for quantifying secondary phase evolution as a function of processing conditions. The semi-quantitative detection of lead-rich phases, such as $(Ca,Sr)_2PbO_4$ and 3221, by means of XRD is also discussed.

II. EXPERIMENTAL

Bi-2223 precursor powders having the overall composition $Bi_{1.8}Pb_{0.3}Sr_{1.8}Ca_2Cu_{3.1}O_x$ were loaded into silver tubes and processed into monofilamentary and multifilamentary tapes using established metallurgical forming techniques [2]. Short lengths of these tapes (typically 3 mm wide, 200 μm thick, and ~25 mm long) were used for the heat-treatment studies. They were annealed in a stainless steel chamber surrounded by a resistively heated furnace with three independently programmable heating zones [10]. Temperatures were monitored using a calibrated Pt/Pt-Rh thermocouple positioned close to the samples and stabilized to $\pm$ 1°C. Samples were ramped up to the desired temperature, held for a specific period of time in 0.075 atm O_2 (total pressure 1 atm, balance N_2), and quenched in silicone oil [5-7].

The XRD measurements were made on peeled sections of monofilamentary tapes and polished sections of multifilamentary tapes using a Rigaku diffractometer with Cu Kα radiation. The lead-bearing phases were quantified using the ratio of the (110) peaks of either Ca_2PbO_4 (d=4.98 Å) or 3221 (d=4.95 Å) to that of the (0010) peak (d=3.08 Å) of the Bi-2212 phase. SEM studies that included EDX and X-ray dot map analyses were performed on transverse sections of tapes that were mounted on epoxy molds, polished, and gold coated for optimum imaging. A JEOL 6400 scanning electron microscope with a Noran Voyager II X-ray Quantitative Microanalysis System was used for this purpose. NIH and Adobe Photoshop software were used for the computer-based image analysis.

III. RESULTS AND DISCUSSION

Figure 1 shows X-ray dot map images of a transverse cross-section of a multifilamentary tape that was heated slowly to 825°C and annealed for 10 minutes in 0.075 atm O_2. From the gray scale image, one can observe two different gray shades among the secondary phases. EDX revealed that the dark gray phase was $(Ca,Sr)_2CuO_3$ (2/1) and the light gray phase was CuO. The X-ray map for calcium clearly correlates the calcium-rich regions with the 2/1 alkaline earth cuprates seen in the gray image. Similarly, the copper-rich regions in the X-ray map for copper correspond well with the gray scale image of the CuO particles. Note that the bismuth, lead, and strontium maps show corresponding deficiencies of these elements in the secondary phase regions as compared to the matrix regions. This is expected, since the matrix has a predominantly Bi-2212 stoichiometry while the secondary phases observed by SEM/EDX tend to be deficient in Bi, Pb, and Sr. X-ray maps for the 14/24 phase in other samples revealed elemental distributions similar to that of CuO except for the fact that the copper map of 14/24 showed intensities that were stronger than those from the matrix but less than those observed for CuO.

Figure 2 shows XRD plots (in the range 2θ=15-20°) for two multifilamentary tapes, A and B, that were heated slowly to 700°C and in 0.075 atm O_2 and then quenched. Both tapes had the same powder stoichiometry but differed in the manner of lead addition. Most of the lead in tape A was in the Bi-2212 phase, whereas most of the lead in tape B was present in the non-superconducting secondary phases. Marker lines 1, 2, and

3 show the location of peaks for the 3221 phase, the Ca_2PbO_4 phase, and the Sr_2PbO_4 phase, respectively [11-13]. The X-ray plots clearly show that tape A contains some 3221 phase (i.e., the single peak at $2\theta=17.89°$), while tape B shows two peaks in that region ($2\theta=17.85°$ and $2\theta=17.69°$) corresponding to the 3221 and Ca_2PbO_4 phases, respectively. (Many researchers have mistakenly identified both of these peaks as belonging to Ca_2PbO_4.) The substitution of strontium for calcium in $(Ca,Sr)_2PbO_4$ shifts the X-ray peaks of Ca_2PbO_4 to lower 2θ values because the strontium cation is larger in size than the calcium cation. Fortunately, the peak for 3221 occurs at a slightly higher 2θ value than the peak for Ca_2PbO_4, thus enabling its unique identification.

The ratios of the intensities of the two peaks for Ca_2PbO_4 and 3221 that occur between 17.5° and 18° to that of the (0010) peak of Bi-2212 gives an indication of the relative amounts of these phases present in a partially or fully processed tape. This methodology can be used for studying the mechanism of lead transfer during the processing of Bi-2223 composite conductors. Since these lead-rich phases are smaller than 1 μm and most EDS systems can not resolve the X-ray peaks for lead and bismuth, it is difficult to positively identify the alkaline earth plumbates and 3221 phase by means of SEM/EDX. Hence, the XRD technique (with slow scanning through the 2θ range of interest) offers a quick and reliable way to overcome this difficulty.

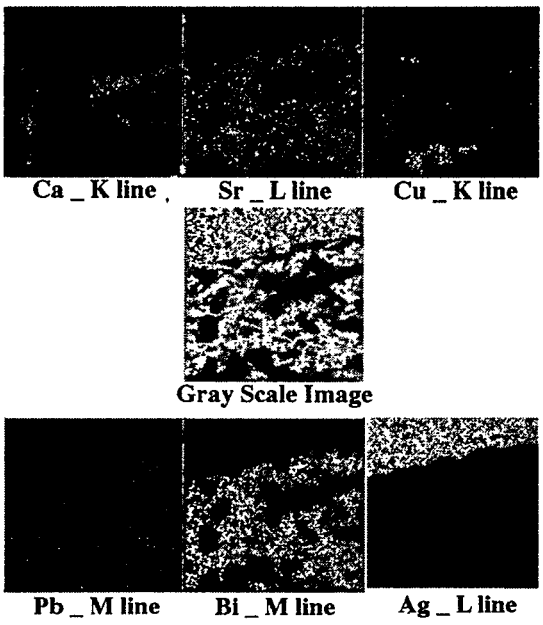

Figure 1. X-ray dot map image of a transverse cross section of multifilamentary tape A, that was annealed at 825°C for 10 minutes in 0.075 atm O_2.

The backscatter electron imaging (BEI) mode can be used to differentiate the secondary phases from voids or cracks. Figure 3 shows SEM micrographs of transverse cross sections of multifilamentary tape B that was heated slowly to 810°C and annealed for 200 minutes in 0.075 atm O_2. Figure 3a shows a BEI micrograph under optimum brightness and contrast conditions. All of the dark gray regions are either secondary phases or voids. Note that the bismuth-rich matrix appears much brighter in the backscatter mode. Figure 3b shows an SEM micrograph of the same cross section at a much higher brightness level. At this brightness level, both the matrix and secondary phases appear to be white; however, a dark band can be seen in the top region. This region contains cracks or voids because there is no electron emission in this region despite using a high-intensity electron beam. This has proven to be a suitable way of differentiating voids from secondary phases. When using scanned SEM images with computer image analysis software for the purpose of secondary phase quantification, it is important to know the location of voids in the micrograph so that these will not be mistakenly quantified as secondary phases.

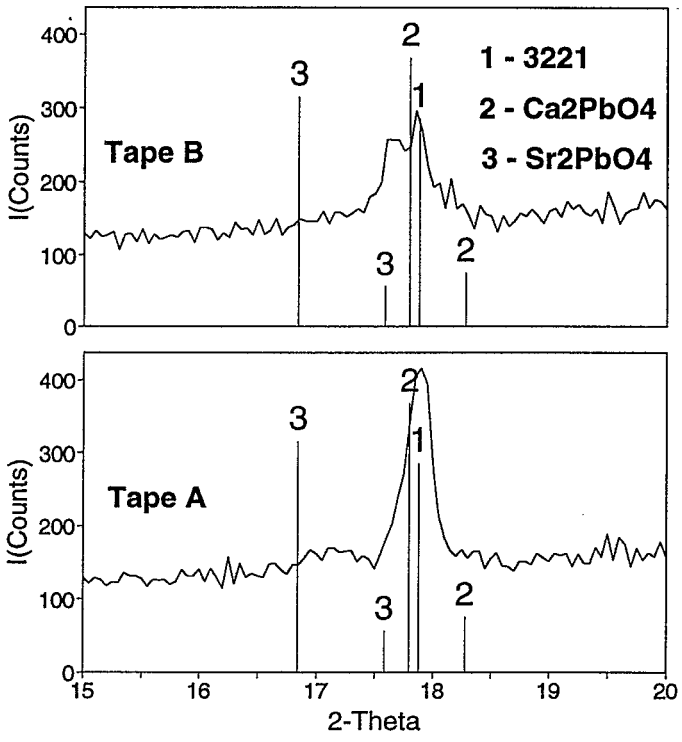

Figure 2. XRD plots for multifilamentary tapes A and B that were heated slowly to 700°C in 0.075 atm O_2 and quenched.

Figure 4 shows a gray scale image of a specimen of tape A that was annealed at 825°C for 10 minutes in 0.075 atm of oxygen. The numbers appearing on each secondary phase particle (dark gray) are computer generated using NIH image analysis software. Since secondary phases, such as CuO and

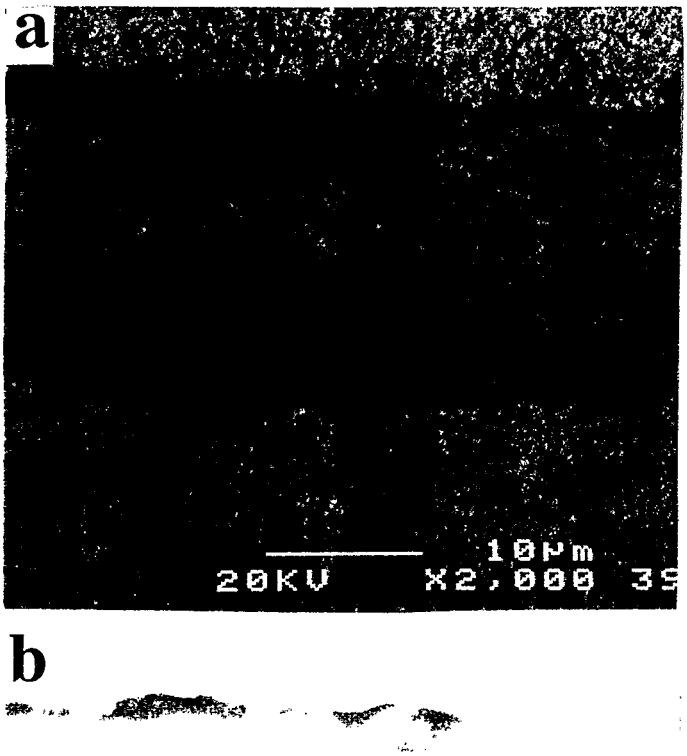

Figure 3. SEM micrographs (backscatter mode) of a transverse section of multifilamentary tape B annealed at 810°C for 200 minutes in 0.075 atm O_2. (a) Low brightness BEI showing secondary phases and voids (gray and black regions) and (b) high brightness BEI showing only voids (gray region).

2/1, have a darker shade than the layered phase matrix, a gray scale window can be selected so as to count only the secondary phase particles. The very dark regions are voids in the sample and have been excluded from the secondary phase analysis. Table 1 lists the area of each particle in Fig. 4. The total matrix area is computed by considering the entire matrix as one particle after excluding the voids. The total secondary phase fraction is then computed as a ratio of the sum of the areas of all 20 particles to that of the total matrix area. In this case we calculate that there is approximately 25% of secondary phase present in the tape. For more accurate computation one must select more regions from the tape cross section and perform a similar analysis. In prior work we introduced such methods for studying the secondary phase content as a function of anneal time, temperature, and pO_2, as described in detail by Luo et al. [7].

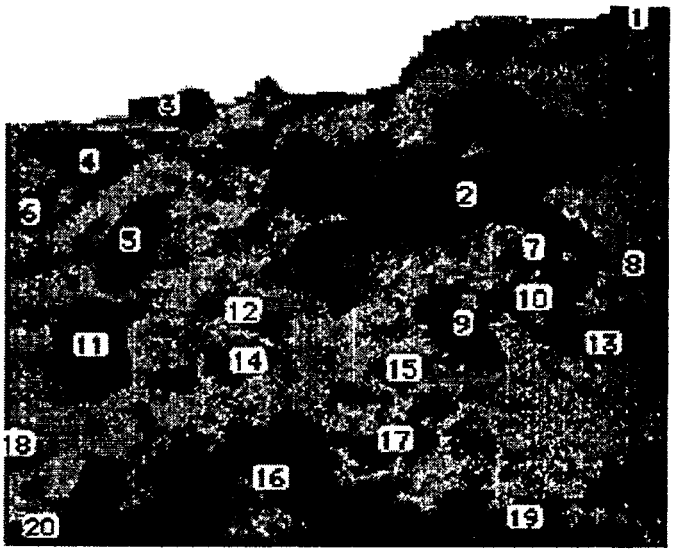

Figure 4. Gray scale image of transverse section of tape A showing secondary particles that have been counted using image analysis software.

IV. SUMMARY

SEM/EDX coupled with X-ray dot mapping, XRD, and computer image analysis methods have been successfully integrated to identify and quantify the secondary phases formed during the processing of $(Bi,Pb)_2Sr_2Ca_2Cu_3O_x$/Ag composite conductors. It has been shown that X-ray dot maps can be used as a convenient means of establishing the presence of secondary phases such as 2/1, $(Ca,Sr)_{14}Cu_{24}O_{41}$, and CuO. XRD analysis can be employed to distinguish lead-rich phases, which are especially prominent during the ramping-up stage of the heat-treatment cycle. Adjusting the brightness level in the backscatter mode of SEM measurements on Bi-2223 composite conductors can serve as a means of distinguishing secondary phases from voids and cracks.

ACKNOWLEDGMENTS

The authors are grateful to Ben Tani and Paul Johnson for their help in obtaining the X-ray maps. The authors gratefully acknowledge J.S. Luo for his critical reading and J. Carr for her editorial assistance. Work at Argonne National Laboratory was sponsored by the U.S. Department of Energy, Office of Energy Efficiency and Renewable Energy as part of DOE program to develop electric power technology, under Contract W-31-109-ENG-38.

Table 1. Area analysis data of various secondary particles shown in Figure 4.

Particle No.	SP area (square μm)	Total area of matrix (square μm)	Area Fraction second phase
1	1.86	---	0.0027
2	63.68	---	0.0927
3	3.57	---	0.0052
4	6.50	---	0.0095
5	7.84	---	0.0114
6	0.86	---	0.0013
7	0.89	---	0.0013
8	2.95	---	0.0043
9	6.11	---	0.0089
10	1.64	---	0.0024
11	11.45	---	0.0167
12	1.71	---	0.0025
13	11.42	---	0.0166
14	1.67	---	0.0024
15	1.19	---	0.0017
16	39.83	---	0.058
17	3.81	---	0.0055
18	1.07	---	0.0016
19	3.64	---	0.0053
20	1.13	---	0.0016
	172.82 total	687	0.252 total

REFERENCES

[1] Y. Yamada, B. Obst, and R. Flükiger, "Microstructural study of Bi(2223)/Ag tapes with J_c (77K, OT) values up to 3.3 x 10^4 A/cm^2, "Supercond. Sci. and Technol. **4**, pp. 165-171, 1991.

[2] K.H. Sandhage, G.N. Riley, Jr., and W.L. Carter, "Critical issues in the OPIT processing of high-J_c BSCCO superconductors," JOM **43**, pp. 21-25, 1991.

[3] K. Sato, N. Shibuta, H. Mukai, T. Hikata, M. Ueyama, and T. Kato, "Development of silver-sheathed bismuth superconducting wires and their application," J. Appl. Phys. **70**, pp. 6484-6488, 1991.

[4] J.S. Luo, N. Merchant, V.A. Maroni, D.M. Gruen, B.S. Tani, W.L. Carter, G.N. Riley, Jr., and K.H. Sandhage, "Thermostability and decomposition of the $(Bi,Pb)_2Sr_2Ca_2Cu_3O_y$ phase in silver-clad tapes," J. Appl. Phys. **72**, pp. 2385-2389, 1992.

[5] N. Merchant, J.S. Luo, V.A. Maroni, S. Sinha, G.N. Riley, Jr., and W.L. Carter, "Effects of oxygen partial pressure on phase evolution and microstructural development in silver-clad $(Bi,Pb)_2Sr_2Ca_2Cu_3O_x$ composite conductors," Appl. Supercond. **2**, pp. 217-225, 1994.

[6] J.S. Luo, N. Merchant, V.A. Maroni, D.M. Gruen, E. Escorcia-Aparicio, B. Tani, G.N. Riley, Jr., and W.L. Carter, "Phase chemistry and microstructure evolution in silver-clad $(Bi_{2-x}Pb_x)Sr_2Ca_2Cu_3O_y$ Wires," IEEE Trans. Appl. Supercond. **3**, 972-975, 1993.

[7] J.S. Luo, N. Merchant, V.A. Maroni, E. Escorcia-Aparicio, B. Tani, G.N. Riley, Jr., and W.L. Carter, "Composition and microstructure evolution of non-supercondcuting phases in silver-clad $(Bi,Pb)_2Sr_2Ca_2Cu_3O_x$ composite conductors," J. Mater. Res. **9**, pp. 3059-3067, 1994.

[8] J.A. Parrell, Y. Feng, S.E. Dorris, and D.C. Larbalestier, "Controlled decompsition and reformation of the 2223 phase in Ag-clad $(Bi,Pb)_2Sr_2Ca_2Cu_3O_x$ tapes and its influence on the microstructure and critical current density," J. Mater. Res. **11**, pp. 555-564, 1996.

[9] N.V. Vo, H.K. Liu, and S.X. Dou, "Effect of sintering periods on the microstructure and electrical transport properties of high-T_c superconducting Bi-(Pb)-Sr-Ca-Cu-O tapes," J. Mater. Res. **11**, pp. 1101-1107, 1996.

[10] N. Merchant, J.S. Luo, V.A. Maroni, D.M. Gruen, B.S. Tani, S. Sinha, K.H. Sandhage, and C.A. Craven, "Epitaxial growth of $YbBa_2Cu_3O_{7-\delta}$ films on (100)-oriented MgO and $SrTiO_3$ substrates by oxidation of a liquid alloy precursor," J. Mater. Res. **7**, pp. 2680-2688, 1992.

[11] S.X. Dou, H.K. Liu, Y. Zhang, and W.M. Bian, "On the new phase $(Bi,Pb)_3Sr_2Ca_2CuO_y$ in the Bi-Pb-Sr-Ca-Cu-O system," Supercond. Sci. Technol. **4**, pp. 203-206, 1991.

[12] J.C. Grivel and R. Flukiger, "A study of the stability of the $(Bi,Pb)_2Sr_2Ca_2Cu_3O_x$ phase in Ag-sheathed tapes," Physica C **235**, pp. 505-506, 1994.

[13] K. Yoshida, Y. Sano, and Y. Tomii, "Precipitation of impurity phases and its effect on the intergrain conducting properties of Ag-doped Bi(Pb)-Sr-Ca-Cu-O," Supercond. Sci. and Technol. **8**, pp. 329-335, 1995.